Intersublattice relaxation of excitons in MnF_2

M. L. J. Hollman, A. F. M. Arts, and H. W. de Wijn
Faculty of Physics and Astronomy and Debye Institute, University of Utrecht, P.O. Box 80.000, 3508 TA Utrecht, The Netherlands
(Received 11 February 1993)

The intersublattice relaxation rate is measured as a function of the temperature for the excitons arising from the ${}^6A_1 \rightarrow {}^4T_1(I)$ transition in MnF_2. It is found that this rate is dominated by scattering with thermal magnons at temperatures above 10 K. The matrix element governing the magnon-induced intersublattice coupling is determined to be 0.086 ± 0.006 cm^{-1}. The relaxation rate at lower temperatures amounts to $(0.75 \pm 0.15) \times 10^6$ s^{-1}, and is consistent with exchange coupling perturbed by the spin-orbit interaction. The low-temperature rate is found to increase by the addition of Zn^{2+} impurities up to concentrations of order 1 at.%.

I. INTRODUCTION

The spectroscopy of excitons and their associated magnon sidebands in antiferromagnetic insulators such as MnF_2 have been intensively investigated and are well understood.[1–4] The subject of exciton dynamics, however, is less well developed. This paper is concerned with the dynamics of the $E1$ excitons, which belong to the ${}^6A_1 \rightarrow {}^4T_1(I)$ transition in MnF_2. These excitons have a very flat band with a dispersion of about 0.01 cm^{-1}, which is much smaller than their inhomogeneous linewidth of 0.5 cm^{-1}.[5] Although an exciton with such a small dispersion is essentially localized on a single ion, it has been shown that these excitons are to a fair degree characterized by a well-defined wave vector.[6]

One of the parameters determining the motion of the excitons is their intersublattice transition rate. This rate was first measured in MnF_2 by Holzrichter, Macfarlane, and Schawlow,[7] who used a technique based on the detection of magnetization changes with the help of a pickup coil. Pumping excitons selectively on one sublattice, they found the intersublattice relaxation rate to amount to about 7×10^5 s^{-1} at a temperature of 2 K. Upon raising the temperature, they furthermore found that this rate increases to roughly 3×10^6 s^{-1} at 15 K. This result was quite naturally ascribed to the scattering of excitons by thermal magnons, though the increase they found lagged markedly behind that of the magnon density.

This paper is devoted to experiments in which we have applied the coil-detection technique to the study of exciton dynamics in MnF_2. The experiments were performed both in nominally pure MnF_2 and in MnF_2 crystals doped with Zn^{2+} ions. Using an experimental setup able to resolve relaxation times in the range between 1 ns and 1 μs, and carrying through a precise deconvolution for the coil response and the laser pulse, we have determined the exciton intersublattice relaxation rate up to temperatures of about 35 K. This extended temperature range permitted us to verify quantitatively the expression for the temperature dependence of the exciton relaxation derived by Ueda and Tanabe[8] as a part of a theoretical study of the influence of the exciton-magnon interaction on exciton motion.

II. EXPERIMENTS

We create exciton-magnon pairs on neighboring Mn^{2+} ions by optical excitation into either the σ_1 or the σ_2 exciton-magnon sideband. This process results mainly in excitons and magnons with large wave vectors, and moreover it is sublattice selective: By proper adjustment of the polarization of the incident light, excitons are created on one sublattice, and magnons on the opposite one. The resultant nonequilibrium populations of free excitons and magnons subsequently relax to their equilibrium distributions by way of intersublattice transitions. The magnetic moments of the excitons and magnons are virtually equal, but of opposite sign. The excitation process thus does not lead to a noticeable change of the total magnetic moment. However, the [001] component of the magnetization, M, changes as a result of the intersublattice transitions, since the exciton and magnon populations relax on quite different time scales.[7,9] These magnetization changes are measured with a pickup coil wound around the sample.

If the magnons and excitons relax with characteristic times τ_m and τ_e, we have

$$M(t) \propto [\exp(-t/\tau_m) - \exp(-t/\tau_e)] \ . \tag{1}$$

Here, we have neglected any delay associated with the dissociation of the exciton-magnon pairs created by the optical pumping. Assuming that the response of the coil circuitry to magnetization changes is monoexponential with a characteristic time τ_c, and that the profile of the laser pulse is specified by $\phi(t)$, we can describe the voltage induced in the coil by

$$V(t) \propto \int_0^t dt' \int_0^{t'} dt'' \, \frac{\exp(-t''/\tau_c)}{\tau_c} \left(\frac{dM(t'-t'')}{dt} \right) \times \phi(t-t') \ , \tag{2}$$

which, upon carrying out the integration over t'', leads to

$$V(t) \propto \int_0^t dt' \left(\frac{\exp(-t'/\tau_c) - \exp(-t'/\tau_m)}{\tau_c - \tau_m} - \frac{\exp(-t'/\tau_c) - \exp(-t'/\tau_e)}{\tau_c - \tau_e} \right) \phi(t-t') \ . \tag{3}$$

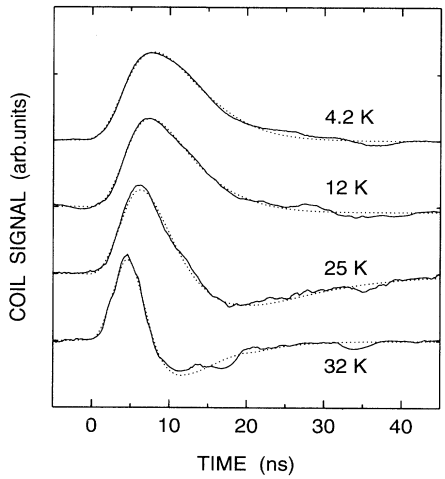

FIG. 1. Typical examples of coil signals as measured at several temperatures between 4.2 and 32 K following optical excitation into σ_1. The dotted lines represent fits of Eq. (3) to the data.

If τ_c and $\phi(t)$ are known, values of τ_e and τ_m can thus be extracted from the measured $V(t)$ by means of numerical deconvolution.

The optical excitation is performed with an excimer-pumped dye laser. This laser generates light pulses in the spectral region around 18400 cm^{-1}, typically with a duration of 10 ns, a peak power of 100 kW, and a spectral width of 0.3 cm^{-1}. The light beam is linearly polarized in an adjustable direction. It propagates through the sample along the c axis and is focused to a waist of about 0.5 mm. The samples are single crystals of MnF_2, both pure and doped with Zn^{2+} up to concentrations of 2.0 at.%. They were grown using the Bridgeman technique. Their dimensions are about $2 \times 2 \times 6$ mm^3, with the longest edges along the c axis, i.e., the preferential axis of the magnetization. The magnetization change along [001] induces a voltage of the order of 1 mV in an eight-turn coil wound around the long axis of the crystal. This voltage pulse is recorded with a fast transient digitizer, and subsequently averaged over typically 1024 traces. The time constant of the coil circuitry was independently measured to be 4.0 ± 0.4 ns. A fast photodiode has been used to record the shape of the laser pulse for each measurement. The minimum resolvable time is about 1 ns, the maximum time around 1 μs.

Some typical examples of coil signals, measured at temperatures between 4.2 and 32 K, are shown as the solid lines in Fig. 1. The small dips observable in the signals at about 16 and 33 ns after the initial rise result from reflections due to residual impedance mismatch in the coil circuitry. The signal at 4.2 K results essentially from magnon relaxation, with a negligible contribution from exciton relaxation. With increasing temperature, the exciton relaxation manifests itself in the coil signal by an increasingly prominent voltage reversal. The dotted lines in Fig. 1 represent least-squares adjustments of Eq. (3) to the data. We see that Eq. (3) provides a faithful representation of the experimental data.

III. RESULTS AND DISCUSSION

In Fig. 2 are shown the measured relaxation rates of the magnetization for excitons created in the decay of the σ_1 sideband in a nominally pure crystal and in MnF_2 crystals doped with 0.5 and 2.0 at.% Zn^{2+}. The data cover about three decades, corresponding to relaxation times from 1 μs down to 2 ns. The decay rates for excitons generated by way of the σ_2 sideband, not shown here, have the same temperature dependence within the experimental errors. This is not surprising, as these excitons presumably decay to the $E1$ level in a time much shorter than the decay time of the magnetization, while conserving their magnetic moment. In an additional experiment, it was found that an external magnetic field along the c axis of the crystal, with a magnitude up to 1 T, has no measurable effect on the decay rates.

It is seen that the exciton relaxation rates are strongly temperature dependent. At temperatures above 8 K, they increase approximately according to a power law of the temperature with an exponent of 3. To explain this power-law dependence, we follow the suggestion[7] that the magnetization decays as a result of transitions from one sublattice to the other, and that the rate increases with the temperature due to a scattering by thermal magnons. In an antiferromagnet such as MnF_2, the spins have antiparallel orientations on the two sublattices. At temperatures so low that no magnons are exited over the magnon energy gap ($\epsilon_{gap}/k_B = 12.54$ K), excitation transfer is only possible between ions located on the same sublattice. Intersublattice transitions then are spin forbidden. In the presence of magnons, on the other hand, exciton intersublattice transitions are allowed, which involve the interchange of an exciton and a magnon on opposite sublattices. An additional argu-

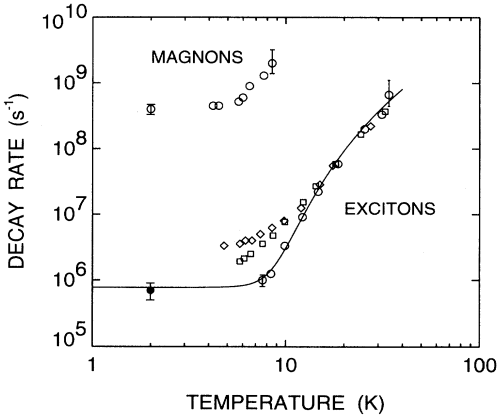

FIG. 2. Exciton magnetization decay rates as function of the temperature for pure MnF_2 (○), and for MnF_2 doped with 0.5 and 2.0 at.% Zn^{2+} (□ and ◇, respectively). Optical excitation is into σ_1. The date point at 2 K is taken from Holzrichter, Macfarlane, and Schawlow (Ref. 7). The solid line is a theoretical fit of Eq. (16) to the data for pure MnF_2. Also shown are the magnon magnetization decay rates for pure MnF_2.

ment that this is the relevant process here is the absence of a magnetic-field dependence. Because the g factors of the excitons and the magnons are nearly equal, such a scattering would stay elastic up to high external fields.

We proceed with a short account of the relevant theoretical results, following Ueda and Tanabe.[8] As a starting point for the derivation we take the Hamiltonian for the exciton-magnon interaction, expressed in terms of the usual local-spin-deviation creation operators $a_j^\dagger$ and $b_l^\dagger$, and the exciton creation operators $A_j^\dagger$ and $B_l^\dagger$, where j and l denote sites on the up and down sublattices, respectively.[3,4,8] That is,

$$\mathcal{H}_{\rm em} = -\sum_{j,l} 2J_{jl}S\left[\epsilon_{jl}(A_j^\dagger A_j a_j^\dagger a_j + B_l^\dagger B_l b_l^\dagger b_l) + \phi_{jl}(A_j^\dagger A_j + B_l^\dagger B_l)(a_j^\dagger b_l^\dagger + a_j b_l) + \rho_{jl}(A_j^\dagger A_j b_l^\dagger b_l + B_l^\dagger B_l a_j^\dagger a_j)\right]$$
$$+\sum_{j,l}\left\{L_{jl}(A_j^\dagger B_l a_j b_l^\dagger + B_l^\dagger A_j b_l a_j^\dagger) + L'_{jl}\left[B_l^\dagger A_j(a_j^\dagger a_j^\dagger + b_l b_l) + A_j^\dagger B_l(a_j a_j + b_l^\dagger b_l^\dagger)\right]\right\} . \quad (4)$$

The coefficients in Eq. (4) are defined by

$$\phi_{jl} = \frac{J'_{jl}}{J_{jl}}\left(\frac{S'}{S}\right)^{1/2} - 1 , \qquad \rho_{jl} = \frac{J'_{jl}S'}{J_{jl}S} - 1 ,$$
$$\epsilon_{jl} = \frac{J'_{jl}}{J_{jl}} - 1 - \frac{(g-g')\mu_B H_A}{2ZJ_{jl}S} , \quad (5)$$
$$L_{jl} = \frac{K_{jl}}{S} , \qquad L'_{jl} = \frac{K_{jl}}{[2S(2S-1)]^{1/2}} ,$$

where the primed quantities refer to the excited state, $S = \frac{5}{2}$, $S' = \frac{3}{2}$, J_{jl} and J'_{jl} are exchange constants, H_A is the staggered anisotropy field, K_{jl} is the matrix element of the intersublattice excitation transfer, and $Z = 8$ is the coordination. We henceforth drop the subscripts in J_{jl}, J'_{jl}, and K_{jl} in Eq. (5), as it is assumed that they are nonvanishing only for neighboring ion pairs jl on opposite sublattices.

The first summation in Eq. (4) represents the magnon-induced modifications of the exciton energy. This part of the exciton-magnon interaction is essentially equivalent to the Hamiltonian describing the scattering of spin waves by impurity ions.[10] The second summation describes exciton intersublattice transitions, and this is the term of interest here. To derive an expression for the exciton intersublattice transition rate from the above Hamiltonian, use is made of the density-matrix formalism, treating the exciton-magnon interaction as a perturbation up to second order. The magnon system is assumed to be in thermal equilibrium. In this way one arrives at two terms providing for the exciton damping. The quantity

$$\Gamma_0 = Z(2JS)^2(Z\epsilon^2\gamma^{(1)} + \phi^2\gamma^{(2)} + \rho^2\gamma^{(1)}) \quad (6)$$

is a measure of the homogeneous broadening of the exciton energy induced by magnon scattering, and

$$\Gamma_1 = Z(2L'^2\gamma^{(3)} + L^2\gamma^{(4)}) \quad (7)$$

is the magnon-assisted intersublattice transition rate we set out to calculate. The parameters $\gamma^{(1)}$ to $\gamma^{(4)}$ are correlation functions between spin-deviation operators.[8]

Following standard linear spin-wave theory, we may write the free-magnon dispersion relation pertaining to MnF_2 as

$$\epsilon_{\mathbf{k}} = 2Z|J|S[(1+\alpha_{\mathbf{k}})^2 - \gamma_{\mathbf{k}}^2]^{1/2} , \quad (8)$$

with

$$\alpha_{\mathbf{k}} = (g\mu_B H_A/2Z|J|S) - (4J_1/ZJ)\sin^2(\tfrac{1}{2}k_z c) , \quad (9)$$
$$\gamma_{\mathbf{k}} = \cos(\tfrac{1}{2}k_x a)\cos(\tfrac{1}{2}k_y a)\cos(\tfrac{1}{2}k_z c) . \quad (10)$$

Here, $J = -1.22$ cm^{-1} and $g\mu_B H_A = 0.76$ cm^{-1}. The second term in the definition of $\alpha_{\mathbf{k}}$ contains the contribution to the magnon energy of the ferromagnetic exchange interaction with the two nearest neighbors along the c axis, with strength $J_1 = 0.22$ cm^{-1}. We have neglected the contribution of this term to the Hamiltonian in Eq. (4), but account is taken of its effect on the dispersion relation and the density of states of the magnons.

The correlation parameters $\gamma^{(1)}$ and $\gamma^{(3)}$ can be expressed in terms of the magnon occupation number per branch $n_{\mathbf{k}}$ as

$$\gamma^{(1)} = \frac{2\pi}{N^2}\sum_{\mathbf{k}}\sum_{\mathbf{k}'}\delta(\epsilon_{\mathbf{k}} - \epsilon_{\mathbf{k}'})n_{\mathbf{k}}(n_{\mathbf{k}'}+1)$$
$$\times(\cosh^2\theta_{\mathbf{k}}\cosh^2\theta_{\mathbf{k}'} + \sinh^2\theta_{\mathbf{k}}\sinh^2\theta_{\mathbf{k}'}) ,$$
$$\gamma^{(3)} = \frac{2\pi}{N^2}\sum_{\mathbf{k}}\sum_{\mathbf{k}'}\delta(\epsilon_{\mathbf{k}} - \epsilon_{\mathbf{k}'})n_{\mathbf{k}}(n_{\mathbf{k}'}+1) \quad (11)$$
$$\times 4\cosh^2\theta_{\mathbf{k}}\sinh^2\theta_{\mathbf{k}'} ,$$

where $\theta_{\mathbf{k}}$ follows from $\tanh 2\theta_{\mathbf{k}} = \gamma_{\mathbf{k}}/(1+\alpha_{\mathbf{k}})$. If we neglect correlations between sites, then $\gamma^{(4)} = \gamma^{(1)}$ and $\gamma^{(2)} = \gamma^{(3)}$. We now introduce the magnon density of states per sublattice

$$\rho(\epsilon) = \frac{1}{N}\sum_{\mathbf{k}}\delta(\epsilon - \epsilon_{\mathbf{k}}) , \quad (12)$$

and the weighted density

$$\rho_c(\epsilon) = \frac{1}{N}\sum_{\mathbf{k}}\delta(\epsilon - \epsilon_{\mathbf{k}})\cosh 2\theta_{\mathbf{k}} . \quad (13)$$

The correlation parameters $\gamma^{(1)}$ and $\gamma^{(3)}$ can then be written

$$\gamma^{(1)} = \pi \int_0^\infty n(\epsilon)[n(\epsilon)+1][\rho_c^2(\epsilon)+\rho^2(\epsilon)]\,d\epsilon\ ,$$
$$\gamma^{(3)} = 2\pi \int_0^\infty n(\epsilon)[n(\epsilon)+1][\rho_c^2(\epsilon)-\rho^2(\epsilon)]\,d\epsilon\ , \tag{14}$$

where $n(\epsilon) = [\exp(\epsilon/k_BT)-1]^{-1}$ is the Bose function.

The expression for the magnon-induced intersublattice rate Γ_1 now becomes

$$\Gamma_1 = K^2\left(\tfrac{4}{5}\gamma^{(3)} + \tfrac{32}{25}\gamma^{(1)}\right). \tag{15}$$

The temperature dependence of Γ_1 is contained in $\gamma^{(1)}$ and $\gamma^{(3)}$. In an antiferromagnet with a negligible anisotropy ($\alpha_{\mathbf{k}} \approx 0$), $\rho(\epsilon)$ would be proportional to ϵ^2 at low energies, and at low temperatures this would lead to a T^3 dependence of $\gamma^{(1)}$ and $\gamma^{(3)}$, and thus of Γ_0 and Γ_1. In the case of MnF_2, however, the anisotropy-associated gap in the magnon density of states for energies below 12.5 K leads to a modification of this temperature dependence.[11]

With the purpose of making a comparison of the measured decay rates with the theory presented above, we have calculated the densities $\rho(\epsilon)$ and $\rho_c(\epsilon)$ for the case of MnF_2, and subsequently performed the integrations in Eqs. (14) for a range of temperatures between 2 and 40 K. The calculations were done numerically. The resulting $\gamma^{(1)}$ and $\gamma^{(3)}$ were substituted in Eq. (15) to obtain Γ_1. The magnetization decay rate equals twice this intersublattice rate, augmented by an additional temperature-independent background rate Γ_{back} due to processes that are not magnon induced. We have compared the resulting decay rate

$$\Gamma = 2\Gamma_1(T) + \Gamma_{\text{back}} \tag{16}$$

with the magnetization decay rates which we measured in pure MnF_2. A least-squares adjustment of Eq. (16) to our data yielded $K = 0.086 \pm 0.006$ cm^{-1} for the matrix element of the intersublattice transfer, and $\Gamma_{\text{back}} = (0.75 \pm 0.15) \times 10^6$ s^{-1}. The corresponding decay rates are shown in Fig. 2 as the solid curve. The background rate is in good agreement with the value from Ref. 7 at 2 K. It is obvious from Fig. 2 that the model excellently describes the data.

A likely candidate for an explanation of the background rate is the spin-orbit coupling. Intersublattice transfer cannot be induced by the exchange interaction alone as the spins have antiparallel orientations on the two sublattices, but will become possible through a second-order perturbation of the relevant wave functions by the spin-orbit coupling. The intersublattice rate associated with this perturbation will be smaller than the intrasublattice coupling ($\sim 10^9$ s^{-1}) by a factor of the order $(\lambda/E_0)^2$, where $\lambda \approx 260$ cm^{-1} is the spin-orbit coupling constant and $E_0 \approx 18400$ cm^{-1} is the exciton energy. This indeed leads to an intersublattice rate of the right order of magnitude.

It appears from Fig. 2 that the residual magnetization decay rate at low temperatures is dependent on the impurity concentration in the crystal. It increases to 3×10^6 s^{-1} in a crystal containing 2.0 at.% Zn^{2+} impurities. We interpret these rates as resulting from transitions in which trapped excitons transfer to a trap on the opposite sublattice, which is associated with the same impurity site. It is well-known[5,12,13] that, because of the very long lifetime of the $E1$ exciton, all created excitons eventually become trapped on Mn^{2+} ions that are perturbed by neighboring impurity ions. Typical trapping rates in a nominally pure crystal are significantly lower than the measured exciton intersublattice rates. Consequently, our experiment in pure MnF_2 reflects the dynamics of free excitons. The addition of Zn^{2+} impurities results in a highly increased exciton trapping rate. We expect that the trapping rate in a crystal doped with 2.0 at.% Zn^{2+} will dominate the intersublattice transition rate, and that all excitons will be trapped within the time scale of the experiment. As a result, our experiment probes the behavior of trapped excitons. The crystal with 0.5 at.% Zn^{2+} represents an intermediate case. The behavior of the excitons at higher temperatures, i.e., above 10 K, appears to be the same in the impure crystals as in the pure crystal. This result is not unexpected: At these temperatures thermal activation by magnons or phonons will cause trapped excitons to scatter back to the free-exciton level, thereby decreasing the effectiveness of the trap.

IV. CONCLUSIONS

We have shown that the technique of the detection of magnetization changes with a pickup coil allows us to follow exciton intersublattice relaxation rates in MnF_2 over almost three orders of magnitude as they increase with the temperature. This temperature dependence is adequately described by a scattering process in which the exciton exchanges sublattices with a thermal magnon. The residual rate at low temperatures presumably is due to a perturbation of the interion exchange interaction by the spin-orbit coupling. In crystals with high impurity concentrations we find an increase in this residual rate.

ACKNOWLEDGMENTS

The authors thank J. P. G. Valkonet for his assistance in taking the data. The support of one of us (M.L.J.H.) by the Foundation "Janivo" is gratefully acknowledged. The work was financially supported by the Netherlands Foundation "Fundamenteel Onderzoek der Materie (FOM)" and the "Nederlandse Organisatie voor Wetenschappelijk Onderzoek (NWO)."

[1] D. D. Sell, R. L. Greene, and R. M. White, Phys. Rev. **158**, 489 (1967).
[2] R. Loudon, Adv. Phys. **17**, 243 (1968).
[3] Y. Tanabe and K. Aoyagi, in *Excitons*, edited by E. I. Rashba and M. D. Sturge (North-Holland, Amsterdam, 1982), Chap. 14.
[4] V. V. Eremenko, Yu. G. Litvinenko, and E. V. Matyushkin, Phys. Rep. **132**, 55 (1986).
[5] R. E. Dietz, A. E. Meixner, H. J. Guggenheim, and M. Misetich, Phys. Rev. Lett. **21**, 1067 (1968); R. E. Dietz, A. E. Meixner, and H. J. Guggenheim, J. Lumin. **1-2**, 279 (1970).
[6] R. M. Macfarlane and A. C. Luntz, Phys. Rev. Lett. **31**, 832 (1973).
[7] J. F. Holzrichter, R. M. Macfarlane, and A. C. Schawlow, Phys. Rev. Lett. **26**, 652 (1971).
[8] K. Ueda and Y. Tanabe, J. Phys. Soc. Jpn. **48**, 1137 (1980).
[9] G. J. Jongerden, A. F. M. Arts, J. I. Dijkhuis, and H. W. de Wijn, Phys. Rev. B **40**, 9435 (1989).
[10] T. Wolfram and J. Callaway, Phys. Rev. **130**, 2207 (1963); T. Tonegawa, Prog. Theor. Phys. **40**, 1195 (1968).
[11] This effect has been observed in a study of the broadening of the pure exciton line by Raman scattering of magnons, a process corresponding to Γ_0 [W. M. Yen, G. F. Imbusch, and D. L. Huber, in *Optical Properties of Ions in Crystals*, edited by H. M. Crosswhite and H. W. Moos (Interscience, New York, 1967), p. 301].
[12] R. L. Greene, D. D. Sell, R. S. Feigelson, G. F. Imbusch, and H. J. Guggenheim, Phys. Rev. **171**, 600 (1968).
[13] B. A. Wilson, W. M. Yen, J. Hegarty, and G. F. Imbusch, Phys. Rev. B **19**, 4238 (1979).